Fe/Cr multilayers: Effect of annealing on the spin structure and magnetoresistance

W. Hahn and M. Loewenhaupt
Institut für Festkörperforschung, Forschungszentrum Jülich, D-52425 Jülich, Germany

G. P. Felcher and Y. Y. Huang
Material Science Division, Argonne National Laboratory, Argonne, Illinois 60439-4845

S. S. P. Parkin
IBM Almaden Research Center, San Jose, California 95120-6099

(Received 7 September 1993; accepted for publication 7 December 1993)

The spin structure of antiferromagnetic Fe/Cr multilayers has been investigated by polarized neutron reflectivity. Measurements were taken on freshly sputtered films as well as films annealed at different temperatures. For annealing temperatures up to 350 °C adjacent Fe layers were found to remain antiferromagnetic, but the coupling strength gradually decreases. In multilayers annealed at higher temperature both antiferro- and ferromagnetic phases are present. In all cases the magnetoresistance is proportional to the amount of antiferromagnetism. The presence of off-specular, diffuse scattering around the antiferromagnetic Bragg peak indicates that the magnetic domains are laterally limited; however, their size is not correlated directly to the magnetoresistance.

I. INTRODUCTION

Fe/Cr is the first and, perhaps, the most widely studied of the class of multilayers that is comprised of alternating thin ferromagnetic layers and nonferromagnetic spacers. For a Cr thickness of 8 Å the Fe layers are coupled antiferromagnetically.[1,2] As the Cr layer thickness is increased, the coupling oscillates from antiferromagnetic (AF), to ferromagnetic (F), and back to antiferromagnetic again.[3] This phenomenon has actually been found to be common for nonferromagnetic metal spacer layers.[4,5] For Fe/Cr the oscillation period is approximately 20 Å. Sandwiches of Fe/Cr/Fe, epitaxially grown in special conditions on single crystal Fe whiskers, show that, in addition, the coupling between Fe layers alternates with the Cr thickness with a period of just 2 Cr monolayers.[6,7] Such periodicity, however, has not been found in multilayers, neither those prepared by sputtering, nor by those prepared by molecular beam epitaxy.

AF coupled Fe/Cr multilayers and sandwiches show an unusual magnetoresistance[3,8,9] whose value oscillates as the spacer thickness is varied, mimicking the oscillations of the antiferromagnetic coupling strength. The absolute value of the magnetoresistance varies greatly with the parameters and method for the sample preparation.[3] Its origin has been attributed to the "roughness" of the interface between Fe and Cr,[10–13] but scant information has been obtained on the scale of such roughness, whether it is local, i.e., composed of one or of a few misplaced atoms, or it consists of wider misaligned plates. Equally obscure is the correlation between a crystalline and a magnetic roughness. For these reasons it was decided to examine the spin structure of Fe/Cr multilayers by polarized neutron diffraction.

Preliminary results were reported together with those on Fe/Gd multilayers in Refs. 14 and 15. Other neutron investigations on Fe/Cr multilayers[16–18] were confined to nonannealed samples. Since the first Bragg reflection of the multilayers occurs at very small angles, close to the region of total reflection, we use "stretched" polarized neutron reflectometry (PNR).[19–21] The main body of the measurements aimed at obtaining the specular reflectivity and, from this, the depth profile of the chemical and magnetic order. Restricting the measurements to a small angle, the relative orientation of the magnetization of subsequent layers are well visible, but not the relative orientation of the magnetic moments in an antiferromagnetic material such as chromium: in this range of scattering angles, chromium appears as nonmagnetic. When roughness is present at the interfaces, the sequence of layers appears as an oscillating, but smoothly varying, profile rather than a periodic sequence of sharp edges. In addition to specular reflection, we observed off-specular scattering in the forward direction; its characteristics enabled us to draw some conclusions of the lateral extension of the magnetic domains composing the multilayers. The measurements were performed on a set of multilayers prepared by sputtering under identical conditions and then annealed at different temperatures. After discussing the main features of the magnetic structure, we will focus on the possible correlation between the structure and the magnetoresistance of annealed Fe/Cr multilayers.

II. EXPERIMENT

A polarized neutron reflectometer is a very simple instrument. A narrow beam of neutrons of wavelength λ hits a sample surface at an angle θ (of the order of 1°) and is reflected at the same angle θ into the detector (see Fig. 1). The intensity of the reflected beam depends on the optical potential of the sample, which is due to the interaction of the neutrons with the nuclei as well as the magnetic fields. The optical potential of the sample modifies the component of the neutron momentum in vacuum, $k_{0z}=2\pi \sin \theta/\lambda$ into

 0021-8979/94/75(7)/3564/7/$6.00

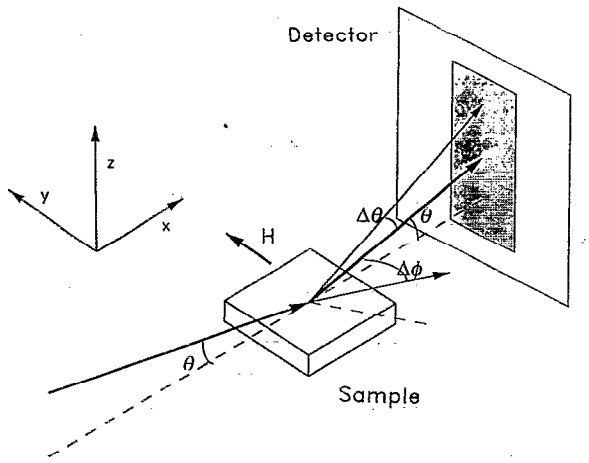

FIG. 1. Geometry of forward and lateral scattering of neutrons at grazing incidence.

$$k_z^{\pm} = \sqrt{k_{0z}^2 - 4\pi(b/V \pm cM_{\parallel})}, \tag{1}$$

where b is the average nuclear scattering amplitude of the medium, V is the average atomic volume, and $M_{\parallel}$ is the component of the magnetization in field direction. $c = 2\pi\mu_n m_n/h^2$ and in convenient units $c = 2.3\times10^{-10}$ Å^{-2}/G. For most materials, b/V is of the order of 5×10^{-6} Å^{-2}. This means that, for a typical neutron wavelength of 5 Å, k_z becomes imaginary at $\theta < 0.35°$, and the neutron beam is totally reflected from the surface.[22] The sign in front of the magnetization $M_{\parallel}$ depends on the polarization of the neutrons relative to the quantization axis **H** (parallel: +; antiparallel: −). For a given spin state, the neutron can be pictured as a unitary wave traveling in vacuum toward the sample which is partially reflected from it with amplitude R^+ or R^-. However, if **M** has a component perpendicular to **H**, the neutron waves must formally include its spin component. Analogous to classical electromagnetism, it has been said that the neutron moment precesses around the local magnetization axis, and the neutron exiting from the surface is polarized in a direction different from the original one.[21,23]

The specular reflectivity is a function of the wave vector transfer perpendicular to the surface, $Q_z = 2k_z$, and it gives patterns whose basic features can be described by simple rules. Since Q_z is a coordinate in reciprocal space, to proceed from the region of small Q_z onward means to pass from a coarse-grained to a more detailed view of the chemical and magnetic profile of the film. Unfortunately, this can be done only at the cost of intensity, since the reflectivity decreases[22] as Q_z^{-4}. When Q_z reaches a value corresponding to the superlattice spacing, the prominent feature of the reflectivity profile is the onset of the first Bragg diffraction peak.

The neutron measurements were taken with the polarized neutron reflectometer POSY I at the Intense Pulsed Neutron Source of Argonne National Laboratory. The samples were positioned between the poles of an electromagnet that provided a magnetic field transverse to the beam and parallel to the sample's surface. The neutrons (of wavelengths ranging from 2.5 to 13.0 Å) were polarized parallel or antiparallel to the magnetic field on the sample. The spin-dependent intensities from a flat sample were measured in a position-sensitive detector at an angle 2θ with the primary beam. The neutron wavelengths were sorted out by the time of flight from the pulsed source to the detector. The reflectivities were determined after normalizing the reflected intensities for the incident spectrum. Practically speaking, this instrument operates like a θ–2θ diffractometer, but with very high resolution ($dQ_z = 0.0004$ Å^{-1}) and limited range (0.004 Å$^{-1} < Q_z < 0.2$ Å^{-1}).

The one-dimensional position-sensitive detector allowed measurement not only of the reflected beam, but also of the neutrons scattered around it. In the scattering geometry sketched in Fig. 1, the one-dimensional detector also identifies neutrons exiting the surface at an angle $\theta_f = \theta + \Delta\theta$ different from the incident angle θ; however, the scattering takes always place in the plane of reflection. In contrast, in the most common geometry of scattering at grazing incidence, the observations are focused on the neutrons scattered *out* of the reflection plane.[24] There is an important difference between the two cases, and thus to avoid confusion we will name the scattering in the plane of reflection as "*forward* scattering" to distinguish it from the lateral scattering at grazing incidence.

In both cases the scattering is due to inhomogeneities in the plane of the multilayer that might be represented by a vector τ with planar projections τ_x and τ_y. In the forward scattering τ_x is obtained from the separation $\Delta\theta$ between the scattered and the reflected beam. In the lateral scattering τ_y is obtained from the angle $\Delta\phi$ between the scattered beam and the reflection plane. When τ is small in comparision to the incoming wave vector, the laws of conservation of energy and momentum in plane reduce to

$$\tau_x = |k| \times \sin\theta \times \Delta\theta$$
$$\tau_y = |k| \times \Delta\phi \quad \left(|k| = \frac{2\pi}{\lambda}\right). \tag{2}$$

For comparable elements $\Delta\theta$ and $\Delta\phi$ the regions of τ_x and τ_y are entirely different. For instance, if $\Delta\theta = \theta = \Delta\phi = 1°$, and a neutron wavelength $\lambda = 10$ Å, $\tau_x = 1.9\times10^{-4}$ Å^{-1}, while $\tau_y = 1.1\times10^{-2}$ Å^{-1}. The difference is about two orders of magnitude. This means that, if the lateral fluctuations τ are isotropic in the plane of the multilayer ($\tau_x = \tau_y$), scattering might be present at a detectable $\Delta\theta$ even when $\Delta\phi$ is negligible small. The size of the objects that gives rise to lateral scattering is the same that gives rise to small angle scattering in transmission geometry; it is of order of 100 Å. The fluctuations that give rise to observable forward scattering are, rather, of the order of 1 μm (10 000 Å).

The samples we investigated were obtained by depositing a total of 30 (Fe 30 Å/Cr 10 Å) bilayers on chemically etched, 1-in.-diam Si(111) wafers, in a high-vacuum dc magnetron sputtering system containing four magnetron sources. The base pressure of the vacuum system prior to deposition was better than 2×10^{-9} Torr. The layers were prepared in 3.2 mTorr of argon at a deposition rate of

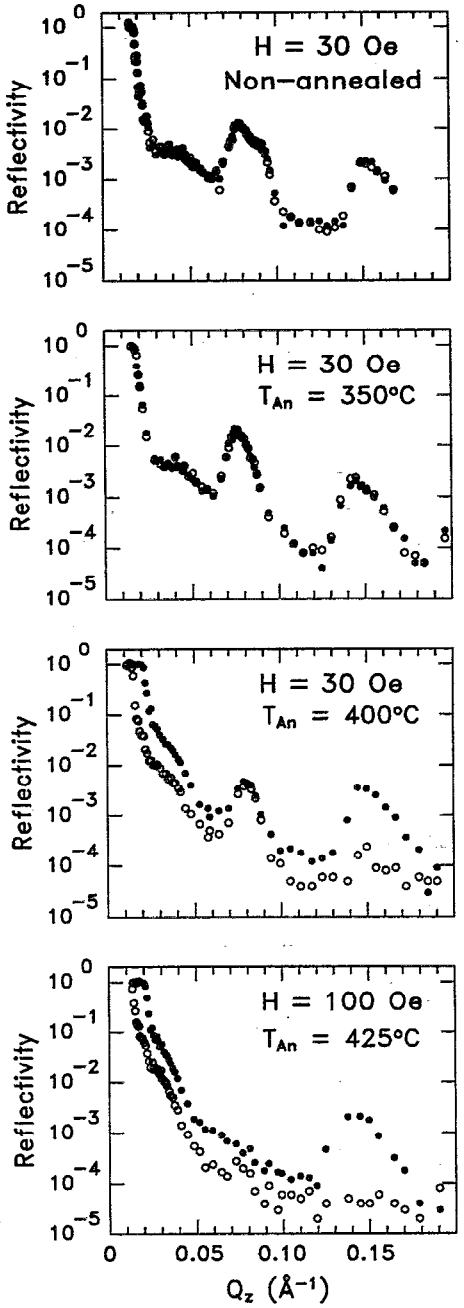

FIG. 2. Spin dependent reflectivities of (Fe 30 Å/Cr 10 Å)×30 multilayers in the virgin state and annealed at different temperatures T_{An} and measured at low fields. (●) and (○) are for neutrons polarized in and opposite to the field direction **H**, respectively.

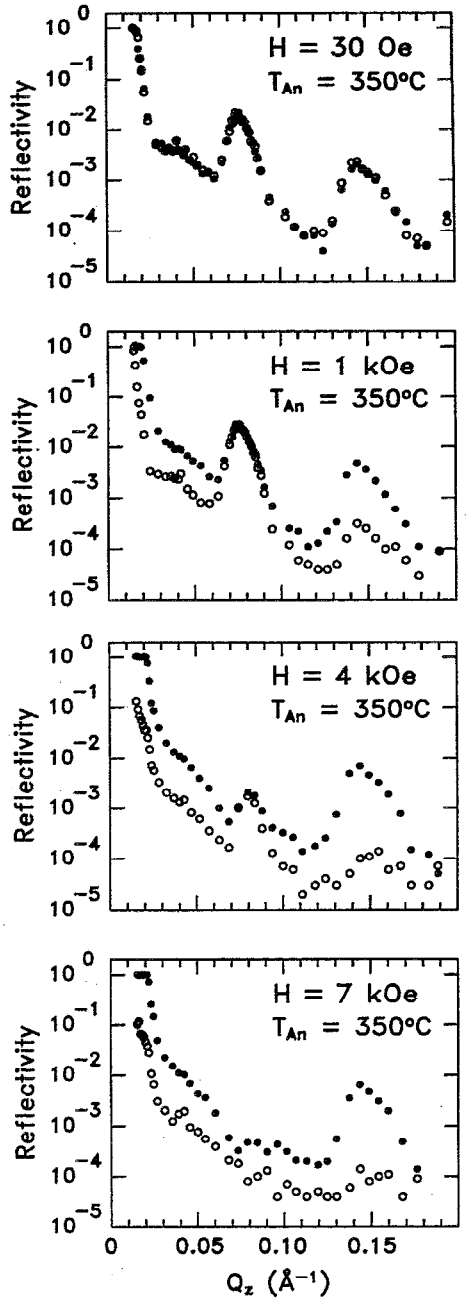

FIG. 3. Spin dependent reflectivities of a (Fe 30 Å/Cr 10 Å)×30 multilayer annealed at 350 °C at different fields. (●) and (○) are for neutrons polarized in and opposite to the field direction **H**, respectively.

2 Å/s with a substrate temperature of 40 °C. Identically prepared samples were annealed for 1 h at temperatures ranging up to 425 °C. All measurements were taken at room temperature.

III. MAGNETIC STRUCTURE

A. "Zero" magnetic field

Figure 2 shows the diffraction patterns in low field for the nonannealed sample and samples annealed at 350, 400, and 425 °C. For annealing temperatures up to 350 °C the net magnetization is zero; the critical edge for total reflection Q_c is spin independent and so is the first structural Bragg reflection at Q_z=0.16 Å^{-1}. The magnetization of the subsequent Fe layers is arranged as in the $+-+-$ sequence, giving rise to the antiferromagnetic (AF) peak at Q_z=0.08 Å^{-1} that is also spin independent. Strictly speaking, the last observation needs to be justified by more than the mere presence of antiferromagnetism of the $+-+-$ kind. It would certainly follow if the sublattice magnetization were perpendicular to the quantization axis of the neutrons. However, if the sublattice magnetization

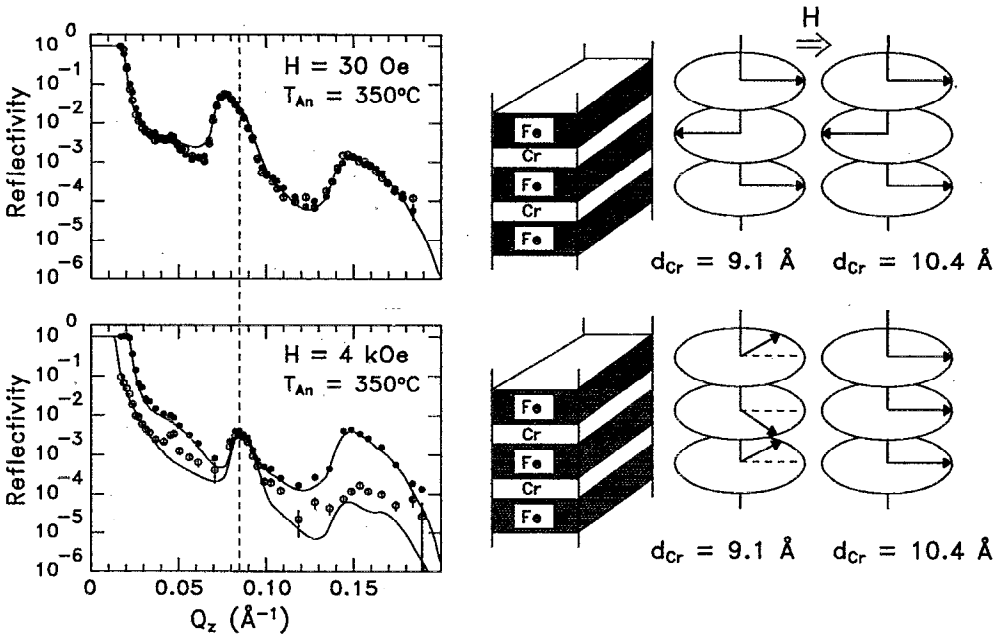

FIG. 4. Left part: spin dependent reflectivities of a (Fe 30 Å/Cr 10 Å)×30 multilayer annealed at 350 °C and integrated over Q_x and Q_y. (●) and (○) are for neutrons polarized in and opposite to the field direction **H**, respectively. For the calculation of the reflectivity, represented by the solid line, we split the sample into two parts with different layer thicknesses and used the spin structures sketched in the right part of the picture.

were parallel to the quantization axis, a magnetic order of the kind $+-+-\cdots$, where the first sign pertains to the surface layer, would be weakly spin dependent, with a preference opposite to that of a $-+-+\cdots$ arrangement. This is because the neutron beam, upon crossing the subsequent layers, is gradually depleted by the partial reflections. When the sublattice magnetization is parallel to the neutron quantization axis, the spin independence of the reflectivity at the AF Bragg reflection is possible only if the sample contains a statistical number of magnetic domains.

For annealing temperatures higher than 350 °C both an AF peak (always spin independent) and an F peak (that is instead strongly spin dependent) are observable. The ferromagnetic component quickly gains with the raising of the annealing temperature, for the 425 °C annealed sample the antiferromagnetic peak is practically absent, and the Fe layers are ferromagnetically coupled.

In an applied magnetic field **H**, a $+-+-$ structure may give rise to both F and AF components. At $H=0$, the antiferromagnetic domains have sublattice magnetizations pointing along one of the crystallographic directions that represent easy axes of magnetization. If the magnetic anisotropy is weak, a modest applied magnetic field is sufficient to flop the sublattice magnetization so as to be perpendicular to **H** in a configuration that assures the highest susceptibility. In fact, the magnetic moments are canted, giving rise to an induced net magnetization proportional to H. Such a description does not apply here. In fields ranging from 10–50 Oe the reflectivities are virtually identical and may be thought of as characteristic of the $H=0$ state.

In conclusion, the simultaneous observation of F and AF components is best interpreted as a due to the fact that, upon annealing, part of the sample remains antiferromagnetic while the remaining becomes ferromagnetic. This does not necessarily mean (and, as a matter of fact, it is not observed) that the regions of magnetic order become smaller, because in the antiferromagnetic state there already exists a large number of magnetic domains.

B. Applied magnetic fields

Figure 3 shows the field-dependent diffraction patterns of a sample annealed at 350 °C. At 30 Oe the net magnetization is zero but for higher fields a ferromagnetic component is present: Q_c and the structural Bragg reflection become spin dependent. At 7 kOe the antiferromagnetic peak has vanished, and the magnetization of all Fe layers is aligned in the direction of the magnetic field. At first sight, a model of canted antiferromagnetism, such as the one described, seems to fit the overall development of the magnetic diffraction pattern. However, a closer look at the response of these samples shows it to be significantly more complex. At 30 Oe both the structural and the antiferromagnetic Bragg peaks show a shoulder on the right-hand side towards the higher Q_z values. At 4 kOe the structural Bragg peak again shows a shoulder on the right-hand side, whereas the antiferromagnetic peak is shifted to higher Q_z values.

The structure in the Bragg peak shows that the periodicity of the superlattice is not uniform over the sample's area. The main part of the sample has a Cr layer thickness of about 10.4 Å, whereas the Cr layer thickness in the remaining part of the sample is only about 9.1 Å. Accepting the idea of a non-homogeneous sample, the widths of

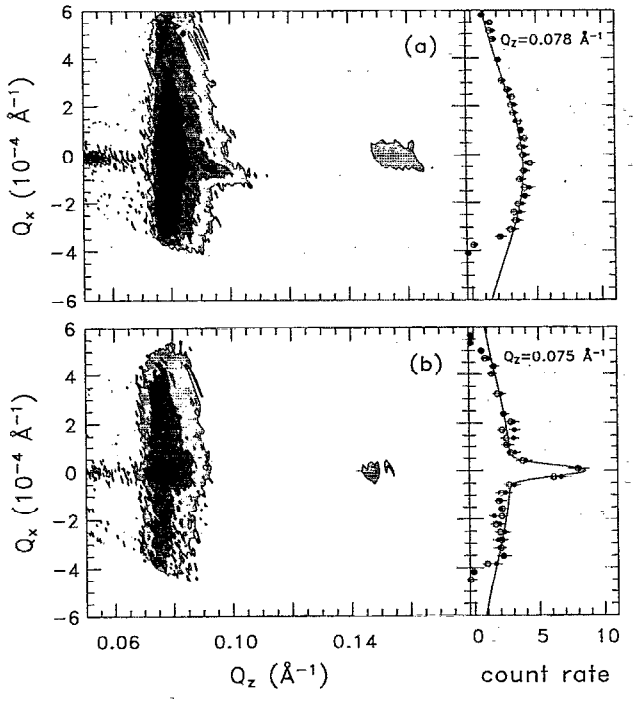

FIG. 5. Left part: intensity contours for the R^+ reflectivity and diffuse scattering from the magnetic domains of the (Fe 30 Å/Cr 10 Å) samples that were (a) not annealed and (b) annealed at 350 °C. Right part: intensity vs Q_x for the given Q_z values and the corresponding figures on the left side.

the structural and AF Bragg peaks were reanalyzed. It was then deduced that the chemical and magnetic correlation lengths perpendicular to the sample's surface were close to the total thickness of the multilayer. X-ray reflectivity measurements, carried out up to angles corresponding to Q_z=0.2 Å^{-1}, fully confirmed the structural analysis described here. The permanence of the AF peak at higher Q_z values with increasing fields shows that, for the part with thinner Cr layers (9.1 Å), the AF coupling is stronger than for the main part of the sample (10.4 Å).

In Fig. 4 we show the result of fitting model calculations to the reflectivity of the 350 °C annealed sample in fields of 30 Oe and 4 kOe. To calculate the reflectivities we use a matrix formalism given in Ref. 23. We split our sample into parts with different periods. Keeping constant the Fe/Cr ratio given nominally for the samples, we chose, basically, two layer thicknesses for Fe and Cr: (Fe 31.2 Å/Cr 10.4 Å) over 77% of the sample and (Fe 27.2 Å/Cr 9.1 Å) over 23% of the sample. The nuclear scattering amplitude densities (b/V) of Fe and Cr were assumed to be the same as in the bulk metals. Finally, the roughness at the interfaces was represented as an error function with an rms roughness of 6 Å. Since a profile containing only the nuclear scattering density was not available, these parameters were not individually refined and are given only as a guide to the work done. The work consisted, basically, in refining the percentages of the two components of different periodicity.

The magnetic scattering length was calculated for a magnetic moment of Fe of 2 μ_B. For an external field of 30 Oe the reflectivities are calculated with a 180° coupling of the Fe layers in all parts of the sample. The sublattice magnetization is assumed to be entirely in the plane of the film, with domains in random directions or (which is equivalent from the point of view of neutron scattering) 50% perpendicular to **H**, 50% parallel to it. In a field of 4 kOe, instead, only the parts of the sample with a Cr layer thickness of 9.1 Å remain partially antiferromagnetic. The magnetization of the Fe layers **M** is at an angle of 30° with **H**, and only a perpendicular projection equal to $\frac{1}{2}$ **M** forms a sequence $+-+-$. In other parts of the sample the Fe moments are entirely aligned to the field. The reflectivities for the different parts of the sample were calculated separately and added by their statistical weight.

The experimental points presented in Fig. 4 are not exactly the same as those in Fig. 3. The reason is that, at around the value of Q_z characteristic of the antiferromagnetic peak, diffuse scattering ($|Q_x|>0$) effectively depletes the reflected beam. In Fig. 4 the diffuse scattering was integrated as best as could be for the geometrically limited neutron counter at our disposal. The result of the fitting is to express in more quantitative terms the notion that sputtered samples are composed of several components of different periodicity and, hence, of different susceptibilities. For this reason it is difficult to describe how the magnetic structure of a well-defined superlattice evolves with the applied magnetic field.

C. Diffuse scattering

Figure 5 shows the intensity contours for reflectivity and diffuse scattering for the (Fe 30 Å/Cr 10 Å) samples in the virgin state (a) and annealed at 350 °C (b). In both cases the external field was 30 Oe. Diffuse scattering occurs only around the AF peak, which is purely magnetic, while it is practically absent at the structural Bragg peak. The diffuse scattering is of magnetic origin and it shows up as a streak along Q_x, at Q_z constant and equal to the antiferromagnetic lattice spacing.

If we assume a simple lateral magnetic structure with a distribution of small magnetic domains, it is easy to calculate the lateral dimensions of the domains with the help of a simple formula. In the kinematic approximation the intensity of the antiferromagnetic peak may be written,[25]

$$J=J_z\times J_x=\frac{\sin^2(N_z a_z Q_z/2)}{\sin^2(a_z Q_z/2)}\times\frac{\sin^2(N_x a_x Q_x/2)}{\sin^2(a_x Q_x/2)}, \quad (3)$$

where, for simplicity, we have neglected fluctuations along y. a_z is the antiferromagnetic spacing and N_z is the number of layers comprising the multilayer. The first term on the right-hand side of Eq. (3) indicates that the maximum of the diffuse scattering always occurs for $Q_z=2\pi/a_z$. In J_x, a_x is, in reality, a dummy parameter; what is of interest is the total length $L_x=N_x a_x$ in the x direction. At the Bragg reflection $Q_x=0$ and the arguments in J_z are multiples of π. At finite Q_x, J_x rapidly decreases. For small Q_x values one can approximate J_x by a Gaussian with a deviation σ, where $\sigma=\sqrt{2\pi}/L_x$ in terms of the total length L_x of the magnetic domains.[25]

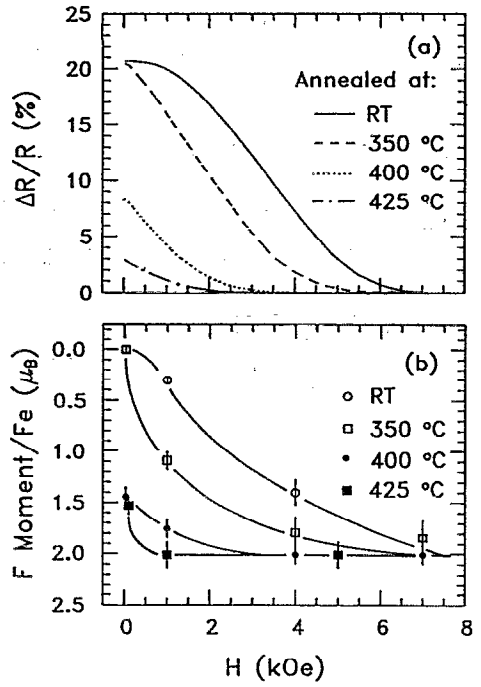

FIG. 6. Magnetoresistance and ferromagnetic (F) moment components of sputtered (Fe 30 Å/Cr 10 Å)×30 multilayers in the virgin and annealed states.

On the right-hand side of Fig. 5 is a cut through the maximum of the AF peaks. The AF peak of the nonannealed sample has only a diffuse component. But, the AF peak of the 350 °C annealed sample separates into a diffuse and a specular reflected component. The half width at half maximum of the diffuse scattering is, in both cases, 0.00045 $Å^{-1}$. The linewidth of the specular reflection is equal to the instrumental resolution (0.00002 $Å^{-1}$). For the structural Bragg peak at Q_z=0.155 $Å^{-1}$ we could not detect any diffuse scattering. In real space the data pertaining to the diffuse scattering translate into the following quantities.

For the virgin sample the average domain size is 0.66 μm for H=30 Oe and increases to 1.0 μm at 1 kOe. The 350 °C annealed sample divides into parts with a domain size of 0.66 μm and another part with a domain size larger than 13 μm (this is actually the limit allowed by our instrumental resolution). If the field is increased from 30 Oe to 1 kOe, the domain size remains constant but the percentage of the diffuse scattering decreases from 90% to 70%. This means that the larger domains are growing at the expense of the smaller domains.

From the practical side, the diffuse character of the antiferromagnetic scattering prevents a better characterization of the direction of the sublattice magnetization by means of polarization analysis. This is conventionally accomplished by inserting, into the reflected beam, a magnetized mirror that reflects one neutron spin state only with reference to the magnetization axis. For a beam scattered over a relatively large range of angles this method is extremely inefficient.

IV. DISCUSSION

We have seen that sputtered multilayers of Fe/Cr are systems that are magnetically (and, by inference, structurally) quite complex. The films contain grains with at least two different superlattice periods, respectively, with a Cr layer thickness of about 9 and 10 Å. From the magnetic standpoint, in the former the antiferromagnetic coupling is stronger. The magnetic domains have a relatively small size in lateral directions and their size actually depends on the annealing conditions and the applied magnetic field. Finally, annealing above 350 °C induces a phase transition over part of the sample which comes to have a ferromagnetic ground state. A question that might be posed is: To what extent do transport properties such as the magnetoresistance depend on the size and the distribution of the grains and of the magnetic domains?

Magnetoresistance as a function of the applied magnetic field is presented for all samples in Fig. 6(a). This is compared in Fig. 6(b) with the net magnetization which is presented upside down to facilitate visual comparison. The magnetization is obtained from reflectivity measurements by measuring the splitting of Q_c for R^+ and R^-. However, we could have also presented the magnetization obtained by conventional means and achieve identical results. The two curves, magnetoresistance and magnetization, are very similar, regardless of the size and number of the magnetic domains. This is particularly evident for the low field values of the virgin sample and that annealed at 350 °C.

In conclusion, we document that the giant magnetoresistance of Fe/Cr superlattices is not directly dependent on the number of magnetic domain boundaries or, overall, on the mesoscopic disorder created by the domain population. This finding lends support to the proposal that the origin of magnetoresistance must be sought at a more microscopic level, in imperfections of some kind at the interfaces of the individual layers.

ACKNOWLEDGMENT

Work at Argonne was supported by the U.S. Department of Energy, Basic Energy Sciences, and Material Sciences, under Contract No. W-31-109-ENG-38.

[1] P. Grünberg, R. Schreiber, Y. Pang, M. B. Brodsky, and H. Sowers, Phys. Rev. Lett. **57**, 2442 (1986).
[2] P. Grünberg, S. Demokritov, A. Fuss, M. Vohl, and J. A. Wolf, J. Appl. Phys. **69**, 4789 (1991).
[3] S. S. P. Parkin, N. More, and K. P. Roche, Phys. Rev. Lett. **64**, 2304 (1990).
[4] S. S. P. Parkin, R. Bhadra, and K. P. Roche, Phys. Rev. Lett. **66**, 2152 (1991).
[5] S. S. P. Parkin, Phys. Rev. Lett. **67**, 3598 (1991).
[6] J. Unguris, R. J. Celotta, and D. T. Pierce, Phys. Rev. Lett. **67**, 140 (1991).
[7] Q. Leng, J. A. Wolf, P. Grünberg, and W. Zinn, in *Physics of Transition Metals*, edited by P. M. Oppeneer and J. Kübler (World Scientific, Singapore, 1993), Vol. 1, p. 434.
[8] M. N. Baibich, J. M. Broto, A. Fert, F. Nguyen van Dau, F. Petroff, P. Etienne, G. Creuzet, A. Friederich, and J. Chazelas, Phys. Rev. Lett. **61**, 2472 (1988).
[9] G. Binasch, P. Grünberg, F. Saurenbach, and W. Zinn, Phys. Rev. B **39**, 4828 (1989).
[10] F. Petroff, A. Barthélémy, A. Hamzić, A. Fert, P. Etienne, S. Lequien,

and G. Creuzet, J. Magn. Magn. Mater. **93**, 95 (1991).
[11] E. E. Fullerton, D. M. Kelly, J. Guimpel, I. K. Schuller, and Y. Bruynseraede, Phys. Rev. Lett. **68**, 859 (1992).
[12] K. Takanashi, Y. Obi, Y. Mitani, and H. Fujimori, J. Phys. Soc. Jpn. **61**, 1169 (1992).
[13] A. Kamijo and H. Igarashi, J. Appl. Phys. **72**, 3497 (1992).
[14] M. Loewenhaupt, W. Hahn, Y. Y. Huang, G. P. Felcher and S. S. P. Parkin, in *Physics of Transition Metals*, edited by P. M. Oppeneer and J. Kübler (World Scientific, Singapore, 1993), Vol. 1, p. 438.
[15] M. Loewenhaupt, W. Hahn, Y. Y. Huang, G. P. Felcher, and S. S. P. Parkin, J. Magn. Magn. Mater. **121**, 173 (1993).
[16] N. Hosoito, K. Mibu, S. Araki, T. Shinjo, S. Itoh, and Y. Endoh, J. Phys. Soc. Jpn. **61**, 300 (1992).
[17] J. A. C. Bland, A. D. Johnson, H. J. Lauter, R. D. Bateson, S. J. Blundell, C. Shackleton, and J. Penfold, J. Magn. Magn. Mater. **93**, 513 (1991).
[18] A. Barthélémy, A. Fert, M. N. Baibich, S. Hadjoudj, F. Petroff, P. Etienne, R. Cabanel, S. Lequien, F. Nguyen van Dau, and G. Creuzet, J. Appl. Phys. **67**, 5908 (1990).
[19] S. S. P. Parkin, A. Mansour, and G. P. Felcher, Appl. Phys. Lett. **58**, 1473 (1991).
[20] C. F. Majkrzak and G. P. Felcher, Mater. Res. Soc. Bull. 65, Nov. (1990).
[21] S. S. P. Parkin, V. Deline, R. Hilleke, and G. P. Felcher, Phys. Rev. B **42**, 10583 (1990).
[22] J. Lekner, *Theory of Reflection* (Matinus Nijhoff, Dordrecht, 1987).
[23] G. P. Felcher, R. O. Hilleke, R. K. Crawford, J. Haumann, R. Kleb, and G. Ostrowski, Rev. Sci. Instrum. **58**, 609 (1987).
[24] H. Dosch, Phys. B **192**, 163 (1993).
[25] R. W. James, *The Optical Principles of Diffraction of X-Rays* (Cornell University Press, Ithaca, 1962).